



The contribution of fires to PM_{2.5} and population exposure in Asia Pacific

Hua Lu¹, Min Xie², Nan Wang³, Bojun Liu⁴, Jinyue Jiang⁵, Bingliang Zhuang⁶, Jianfeng Yang⁷,
Kunqin Lv⁸, Danyang Ma²

¹ Chongqing Institute of Meteorological Sciences, Chongqing 401147, China

² School of Environment, Nanjing Normal University, Nanjing 210023, China

³ College of Carbon Neutrality Future Technology, Sichuan University, Chengdu 610065, China

⁴ Chongqing Meteorological Observatory, Chongqing 401147, China

⁵ The First Affiliated Hospital of Chongqing Medical University, Chongqing 400010, China

⁶ School of Atmospheric Sciences, Nanjing University, Nanjing 210023, China

⁷ The People's Hospital of Kaijiang, Dazhou 636250, China

⁸ The First People's Hospital of Jiangjin District, Chongqing 402260, China

Correspondence to: Min Xie (minxie@njnu.edu.cn) and Nan Wang (nan.wang@scu.edu.cn)

Abstract. Forest and vegetation fires are one of the major sources of air pollution and have triggered air quality issues in many regions of Asia. Measures to reduce fires may be a significant yet under-recognized option for efficiently improving air quality and averting the related premature deaths. Here we isolate the fire-specific PM_{2.5} from monitoring concentrations using an observation-driven approach in the region. Fire-specific PM_{2.5} concentrations average 2-15 µg/m³ during the fire season, with higher values in Southeast Asia (ESA), Northeast Asia (NA), and northern India. The total PM_{2.5} in Asia Pacific exhibits a rapid declining trend from 2014 to 2021, while fire-specific PM_{2.5} decreases in early years but begins to reverse in ESA and NA. The proportions of fire-specific PM_{2.5} in NA rises from 0.2 to 0.3 during the fire season, and in ESA increases from 0.2 in 2018 to 0.4 in 2021. Fire-specific PM_{2.5} exposure caused 58,000, 90,000, 157,000, and 29,300 premature deaths annually in ESA, East Asia (EA), Central Asia (CA), and NA, respectively, accounting for 40.9%, 14.9%, 19.4%, and 24.1% of numbers caused by the total PM_{2.5}. Analysis of infant mortality rate data and PM_{2.5} exposure indicates that the total PM_{2.5} exposure impacted more in richer areas, while fire-specific PM_{2.5} exposure affected more populations in poorer regions. Based on the positive correlation between VPD and fire-specific PM_{2.5}, this study suggests that without further regulation and policy intervention, the emerging growth trend of fire-specific PM_{2.5} in Asia Pacific is likely to continue under the influence of future climate change.



31 **1 Introduction**

32 $PM_{2.5}$ is a complex mixture of anthropogenic and natural sources, and has been the world's
33 leading environmental health risk factor (McDuffie et al., 2021). Observations show that
34 emissions from forest and vegetation fires are one of the major sources of PM and have triggered
35 air quality issues in many regions (Reddington et al., 2021; Romanov et al., 2022; Xie et al., 2022).
36 Influenced by climate change, fires are becoming increasingly frequent and destructive, and
37 fire-specific $PM_{2.5}$ has begun to dominate the average annual $PM_{2.5}$ trends in some areas (Marshall
38 et al., 2023; Wei et al., 2023). Compared with the direct exposure to flames and heat of fires,
39 exposure to fire smoke can affect much larger populations and pose significant public health risks
40 (Xu et al., 2023a). The most severe public health impact of fire smoke on air pollution comes from
41 the generation of toxic PM. Recent studies suggest that fire-specific $PM_{2.5}$ may be more influential
42 than equal doses of ambient $PM_{2.5}$ (Xue et al., 2021; Aguilera et al., 2023; Wei et al., 2023).
43 Exposure to fire-specific $PM_{2.5}$ can exacerbate a range of health problems, such as premature
44 mortality, cardiovascular and respiratory and other health issues (Aguilera et al., 2021; Chen et al.,
45 2021).

46 Asia Pacific is one of the most densely populated regions in the world and faces severe air
47 pollution challenges (CCAC, 2024). Among the health risks associated with air pollution, Asia
48 Pacific has accounted for over 70% of global deaths attributed to air pollution (Lelieveld et al.,
49 2015; 2020; Giannadaki et al., 2018). Fire activity in the North Asia (NA) region has recently
50 become more extensive and is expected to continue escalating in the future due to climate change
51 (Huang et al., 2024; Gui et al., 2024). Fires in equatorial Southeast Asia (SEA) are severely
52 impacted by droughts induced by the El Niño-Southern Oscillation (Yin et al., 2020; Zheng et al.,
53 2023). South Asian are among the most vulnerable globally to the impacts of climate change,
54 which has increased the incidence of fire in South Asia (SA). In addition to climate and natural
55 factors, the frequencies and sizes of fires are also largely human influenced through land
56 management practices in Asia Pacific. In East Asia (EA) and SEA, fires are used as agricultural
57 management tools, such as to remove agricultural residues and weeds, as well as for forest
58 clearance for agricultural purposes (Biswas et al., 2015; Phairuang et al., 2017). Fire activity in
59 Asia Pacific may release large amounts of smoke and harmful gases, leading to elevated



60 concentrations of air pollutants and negatively affecting human health and the environment
61 (Reddington et al., 2021). The fire-specific air pollution in Asia Pacific not only poses a threat to
62 the health of local residents but can also influence neighboring areas and even more distant
63 locations through atmospheric transport (Zhu et al., 2016; Qin et al., 2024; Du et al., 2024).

64 However, large disparities in geographic patterns exist in fire-specific air pollution and
65 population exposure researches, with related studies most centralized in high-income economies,
66 like North America and Europe (Aguilera et al., 2021; Tornevi et al., 2021; Korsiak et al., 2022;
67 Wei et al., 2023). In contrast, the world's most widely burnt regions, including the Asia Pacific,
68 remain underrepresented in literature due to resource inequality and inadequate funding (Petersen,
69 2021; Lin et al., 2024). On one hand, a major challenge to conduct researches on fire-related $PM_{2.5}$
70 pollution and population exposure is how to isolate the fire-specific $PM_{2.5}$ from observed
71 background levels. More than 70% of studies on fire-related datasets are concentrated in North
72 America and Europe, using various approaches such as chemical transport models, satellite-based
73 fire smoke plume analysis and statistical approaches to quantify fire-specific $PM_{2.5}$ (Aguilera et al.,
74 2021; Schneider et al., 2021; Korsiak et al., 2022; Wei et al., 2023; Lin et al., 2024). However,
75 there is still a lack of fire-specific $PM_{2.5}$ in many other regions, including Asia Pacific, which
76 accounts for 7.4% of the global burnt area and 27% of global cropland fires (Xu and You, 2023;
77 Xu et al., 2023). on the other hand, associated with the socioeconomic factors, increasing evidence
78 highlights the unequal distribution of exposure to and impacts of air pollution, attributed to the
79 disparities in the implement of measures, effectiveness of regulations, the adoption of clean
80 energy technologies, and differences in infrastructure and healthcare conditions (Tessum et al.,
81 2019; Jbaily et al., 2022; Kodros et al., 2022; Southerland et al., 2021; Rentschler et al., 2023).
82 However few studies have focused on how fire-specific $PM_{2.5}$ exposure manifests along lines of
83 inequality, thereby exacerbating health disparities. Notably, there is a lack of research focusing on
84 contributions of fires activities to $PM_{2.5}$ in Asia Pacific, as well as the health and socioeconomic
85 impact of fire-specific $PM_{2.5}$.

86 This study utilized a trajectory-fire interception method (TFIM), and spatial-temporal interpolations
87 through machine learning algorithm to isolate fire-specific $PM_{2.5}$ from monitoring observations in Asia
88 Pacific. With the fire-specific $PM_{2.5}$, variations in contributions of fire activities to $PM_{2.5}$ in the
89 Asia Pacific are analyzed. The health impacts caused by fire-specific $PM_{2.5}$, and the relationship



90 between poverty levels and fire-specific $PM_{2.5}$ exposure in Asia Pacific were also examined.
91 Based on the climate factors related to fire activities, this study aims to demonstrate whether the
92 changing trends of fire-specific $PM_{2.5}$ will go on due to climate change.

93 **2 Data and Methods**

94 **2.1 Data**

95 2.1.1 Air quality Data

96 The continuous air quality observation data were obtained from the OpenAQ website
97 (<http://openaq.org/>), while data for the China region primarily comes from the Chinese National
98 Environmental Monitoring Center (<http://www.cnemc.cn/en/>). The total $PM_{2.5}$ between 2014 and
99 2020 were measured using observation data from 1,810 monitoring stations (Figure 1) located
100 throughout the Asia Pacific (65-133°E, 5-55°N). Additionally, the CO measurements from these
101 monitoring stations were utilized to validate the definition of fire influence using the TFIM
102 method.

103 2.1.2 Fire Point Data

104 The location of fires were obtained from the Fire Information for Resource Management
105 System (FIRMS). Rrchived fire pixels from the Moderate Resolution Imaging Spectroradiometer
106 (MODIS) on the Aqua and Terra satellites for Asia Pacific from 2010 to 2021 were downloaded.
107 The standard fire products with a resolution of 1 km×1 km for each fire pixel were utilized. More
108 information about MODIS measurements can be found in Giglio et al. (2003) and Justice et al.
109 (2011).

110 2.1.3 Additional Variables

111 To estimate fire-specific $PM_{2.5}$ concentrations, the study firstly used spatial-temporal
112 interpolation approach to calculate counterfactual $PM_{2.5}$ that is in absence of fire smoke. The
113 spatial-temporal interpolation approach was realized based on a machine learning methods with
114 multiple potential explanatory variables, including aerosol optical depth (AOD) data,
115 meteorological data, land use data, and other auxiliary information.

116 For AOD data, the reliability of the MODIS products onboard the U.S. Terra and Aqua
117 satellites has been extensively validated. The high resolution AOD product, with a resolution of 1



118 km, is derived using the Multi-Angle Implementation of Atmospheric Correction (MAIAC)
119 algorithm, which enhances the accuracy and spatial resolution of the AOD product (Lyapustin and
120 Wang, 2018). The MAIAC AOD data has recently been widely applied to retrieve ground-level
121 $PM_{2.5}$ concentrations (He et al., 2020; Li et al., 2020; Wei et al., 2023).

122 Satellite remote sensing offers uniform coverage, but satellite data is only feasible under
123 clear-sky conditions. MAIAC AOD contains large data gaps due to ubiquitous presence of clouds.
124 To fill spatial-temporal gaps of MAIAC AOD, this study also supplemented MERRA-2 AOD
125 products. MERRA-2 is the first global reanalysis dataset of the satellite era, provided by NASA's
126 Modeling and Assimilation Data and Information Services Center. It assimilates ground-based
127 aerosol observations, with a horizontal resolution of $0.625^\circ \times 0.5^\circ$ and a temporal resolution of 1
128 hour (Gelaro et al., 2017). Studies have used MERRA-2 aerosol products to conduct in-depth
129 researches on atmospheric environmental issues in Asia (Jia et al., 2019; Feng et al., 2020).
130 Additionally, MERRA-2 provides 50 aerosol products, including AOD, surface black carbon mass
131 concentration, surface organic carbon mass concentration, and surface dust mass concentration.
132 This study utilizes MERRA-2 reanalysis aerosol products as input data for constructing the
133 AOD- $PM_{2.5}$ model.

134 Meteorological variables affect air pollution, therefore meteorological data provided by ERA5
135 reanalysis data serve as input factors for estimating the $PM_{2.5}$ in absence of fire smoke. ERA5
136 reanalysis data comes from ECMWF and assimilates as comprehensive observational data as
137 possible (including ground observations, soundings, aircraft data, satellite observations, etc.). It is
138 widely used in weather and climate-related research, with a horizontal resolution of $0.25^\circ \times 0.25^\circ$
139 and divided into 37 vertical layers, with a resolution of 25 hPa from 750 to 1000 hPa and 50 hPa
140 from 750 to 250 hPa, and a temporal resolution of 1 hour. The data used in the study included
141 surface air pressure, 10-meter U and V wind fields, 2-meter temperature and dew point
142 temperature, as well as specific humidity and temperature at 500 hPa and 850 hPa.

143 Land-use variables are proxies for emissions and background $PM_{2.5}$. In this study, the land-use
144 coverage types collected from the MCD12Q1 Version 6 products, and the 16-day composite
145 Normalized Difference Vegetation Index (NDVI) derived from MODIS were utilized as input
146 factors for $PM_{2.5}$ estimation. In addition, the population density obtained from LandScan was
147 included to represent impact of human activities on air pollution.

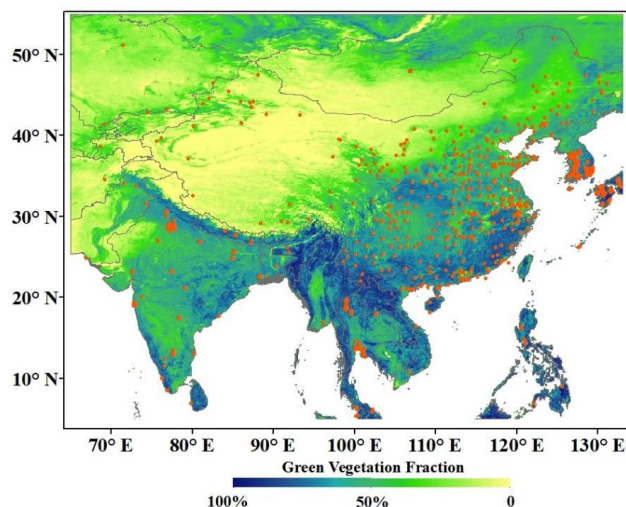


2.1.4 Health Data

To estimate the health impacts at a specific ambient $PM_{2.5}$ exposure, population data from LandScan and mortality rate data from the online Global Burden of Disease (GBD) database (<http://ghdx.healthdata.org/gbd-results-tool>) covering Asia Pacific from 2014 to 2020 were collected and used. The GBD database provides baseline mortality data for male and female populations across five-year age groups. This study considers health endpoints for four diseases: stroke (STROKE), chronic obstructive pulmonary disease (COPD), ischemic heart disease (IHD) and lung cancer (LC).

2.1.5 Infant Mortality Rates

The Infant Mortality Rates (IMR) dataset from NASA Socioeconomic Data and Applications Center was used as a proxy for population poverty levels in this study. The IMR is defined as the number of children who die before their first birthday for every 1000 live births in a given year (Barbier and Hochard, 2019; Reddington et al., 2021). IMR dataset has been widely used as poverty indicators, with specific thresholds to assess and categorized poverty levels (Barlow et al., 2016; Barbier and Hochard, 2019). This study define population with $IMR \leq 40$ to be relatively not poor, $41 \leq IMR \leq 60$ to be moderately poor, $IMR \geq 61$ to be relatively poor, which is similar to the definition in Barbier and Hochard (2019).



165

166 **Figure 1.** Distribution of air quality monitoring stations in Asia Pacific, with shading color in
167 background indicating green vegetation fraction.



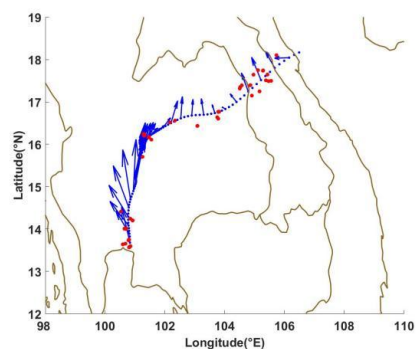
168 2.1.6 The Coupled Model Intercomparison Project Phase 6 data

169 Referring to previous researches, a positive relationship may exist between the vapor
170 pressure deficit (VPD) and the fire-specific $PM_{2.5}$ (Abatzoglou et al., 2016; Burke et al., 2023). To
171 validate this relationship and quantify the future trend of fire-specific $PM_{2.5}$ in Asia Pacific, VPD
172 was calculated using the projected temperature and relative humidity data from climate model
173 (GCM) ensembles under various emissions scenarios. The study examined VPD changes under
174 three commonly used climate scenarios (SSP1-2.6, SSP2-4.5, and SSP3-7.0), based on monthly
175 data provided by 34 GCMs. To minimize uncertainty and account for internal variability, the
176 average VPD values for different regions in Asia Pacific were computed for each GCM and
177 emissions scenario.

178 **2.2 Methods**

179 2.2.1 Fire Influence definition

180 To understand how fire impact air quality, whether an ambient $PM_{2.5}$ measurement has been
181 influenced by fire should be determined. Following the TFIM method proposed by Schneider et al.
182 (2021), this study calculated the backward trajectories for monitoring stations over a 72-hour
183 period. The FLEXPART model (version 10.4), a Lagrangian particle dispersion model developed
184 by the Norwegian Institute for Air Research, was used for back-trajectories calculation.
185 FLEXPART v10.4 was driven using ERA5 reanalysis data at a temporal interval of 1 hour. These
186 trajectories were then spatially and temporally matched with fire hotspot data reported by FIRMS.
187 If the distance between the two was within 0.5° , an interception was considered to occur. If a
188 trajectory had more than the interception threshold, the $PM_{2.5}$ measurement at that time was
189 deemed to be influenced by fire. A schematic of the TFIM method is shown in Figure 2.



190

191 **Figure 2.** The schematic of trajectory-fire interception method (TFIM), where the blue lines
192 represent backward trajectories and red points indicate fire hotspots

193 2.2.2 Fire-specific $PM_{2.5}$ estimation

194 To estimate fire-specific $PM_{2.5}$ covering Asia Pacific from 2014 to 2020, the counterfactual
195 $PM_{2.5}$ unaffected by fire was interpolated through machine learning method, and then compared
196 with the ambient $PM_{2.5}$ measurement to get the fire-specific $PM_{2.5}$. The specific steps in Figure 3
197 were followed. Since there are no direct fire smoke observation data over Asia Pacific, the TFIM
198 method described in 2.2.1 was used as a substitute. First, using the TFIM method, the fire
199 influence periods for a given monitoring station time were determined. If a station experienced
200 over 6 hours of fire influence in a day, it was considered exposed to fire smoke on that day. Based
201 on the exposure definition, the station days exposed to fire were temporarily removed. Next, the
202 random forest method was employed to interpolate non-fire-affected $PM_{2.5}$ for all station days
203 categorized as fire-affected. This step provided background $PM_{2.5}$ estimation unrelated to fire
204 contributions. The $PM_{2.5}$ from non-fire-affected station days was used as the training, testing, and
205 validation datasets to build the model, and interpolation estimation was performed for background
206 $PM_{2.5}$ for fire-affected station days. Finally, by subtracting the non-fire-affected part from the
207 ambient $PM_{2.5}$ measurement, the fire-specific $PM_{2.5}$ was estimated.

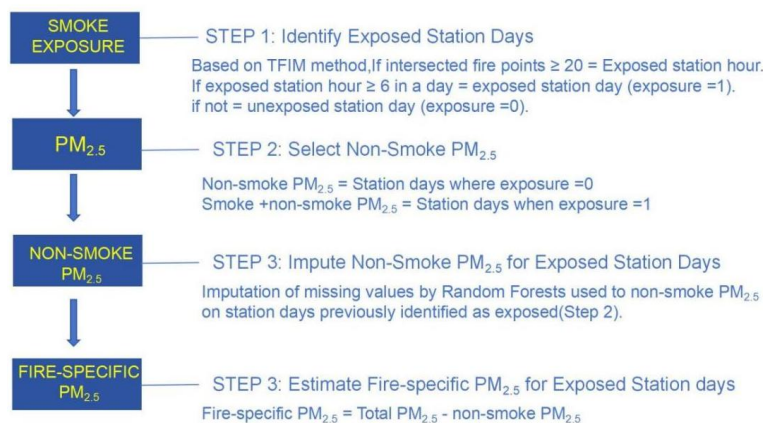


Figure 3. Flowchart of steps followed to estimate fire-specific PM_{2.5}

2.2.3 PM_{2.5} health impact assessment

The disease burden attributable to PM_{2.5} exposure was assessed using Health Impact Function (HIF). The expression for this function is as follows:

$$\Delta Mort = B_i \times POP \times (1 - 1/RR_i)$$

where $\Delta Mort$ denotes the premature death due to PM_{2.5} exposure for health endpoint i , B_i represents mortality rate for endpoint i , POP is the exposed population, and RR_i is the relative risk associated with PM_{2.5} exposure for health endpoint i .

With the advancement of epidemiological research, an Integrated Exposure-Response (IER) equation integrates available RR information from multiple exposure-response functions, including air pollution, active smoking, passive secondhand smoke exposure, and indoor cooking fuel combustion scenarios. The IER equation combines findings from studies on both low and high exposure concentrations to consider four major health endpoints (STROKE, COPD, IHD, and LC). The expression for the IER has the following form:

$$RR = 1 + \alpha(1 - \exp(-\gamma(C - C_0)^\delta))$$

Where C represents the PM_{2.5} concentration, C_0 is the concentration threshold below which health risks are negligible, and the parameters α , γ and δ represent the fitted parameters for health endpoint i to describe the relative risk curve. The values for parameters can be found in studies by Burnett et al. (2014) and Song et al. (2017).



226 **3 Results**

227 **3.1 Estimating fire-specific PM_{2.5}**

228 Fire hotspots number derived from the FIRMS products in Asia Pacific peaked during
229 February to April (with daily counts exceeding 1000), therefore we defined this period as fire
230 season in this study (Figure 4). In terms of spatial distribution, fire hotspots number in ESA is
231 more than double that of the other three regions during fire season. Fires in ESA mainly occur
232 during the pre-monsoon period (roughly February to April), due to widespread forest fires and
233 agricultural residues burning in preparation for planting before the arrival of the Asian summer
234 monsoon (Huang et al., 2017; Phairuang et al., 2017). The increase in fire activity coincides with
235 the establishment of stable temperature inversions over large areas of Thailand, Vietnam, Laos,
236 and southern China, while northern Thailand experiences hot, dry, and calm conditions that
237 facilitate the formation of haze (Reddington et al., 2021). Fire activities significantly decrease
238 after the onset of summer monsoon rainfall (in late April) and remain low until the beginning of
239 the dry season (in November). The fire occurrences in this region exhibit a certain degree of
240 interannual variability (Figures 4c and 4d), which is related to changes in atmospheric circulation
241 patterns, such as the India-Burma trough (Huang et al., 2017). In addition to climatic influences,
242 local fire management policies also play a role; for example, the implementation of stricter
243 agricultural burning policies in ESA mainland between 2016 and 2017 was associated with a
244 significant reduction in fire point counts. However, after 2018, the number of fire points once
245 again showed an upward trend.

246 Fire hotspots number in CA is slightly higher than EA during the fire season (Figures 4b and
247 4d). The dry and hot conditions before the monsoon in CA create favorable conditions for forest
248 fires in the dense vegetation of the Indian Peninsula. Additionally, the dry winter climate in CA
249 can also contribute to fire occurrences (Barik and Baidya, 2023). As a result, the peak fire point
250 counts in CA primarily occur in March-April and October-November. The climate conditions in
251 EA are complex. During spring and autumn, North China and Southwest China experience clear
252 weather, low precipitation, and dry vegetation, making them prone to forest fires, especially
253 during windy conditions. In the western Xinjiang region, the peak period for forest fires is
254 concentrated in the summer, particularly those caused by lightning, with a significant number



255 occurring in July-August. The Northern Asia (NA) region is located relatively further north, with
 256 the start of the growing season (SOS) lagging behind the other three regions, while the end of the
 257 growing season (EOS) occurs earlier than in the other regions. As a result, the peak fire point
 258 period in NA is delayed in spring (March-May) compared to the other three regions, but slightly
 259 advanced in autumn. The average daily number of fire points in CA, EA, and NA has shown a
 260 slow increasing trend from 2014 to 2021.

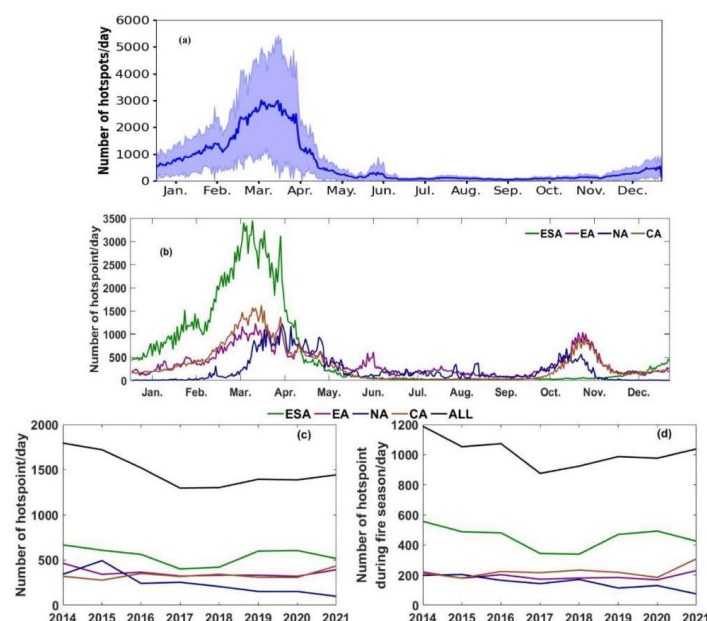
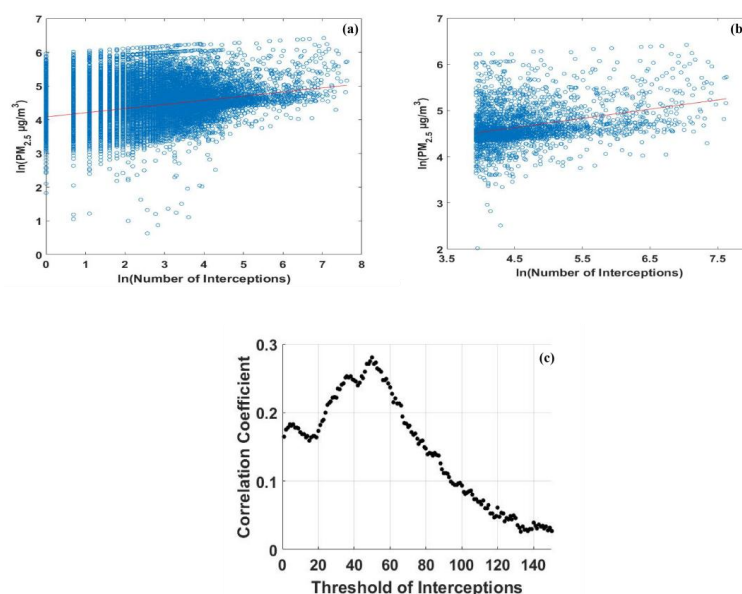


Figure 4. The distribution of fire hotspots in Asia Pacific from 2014 to 2021.

263 To isolate the fire-specific $PM_{2.5}$ based on TFIM, we should firstly justify the usability of
 264 TFIM in the Asia Pacific, and then set a suitable threshold of fire hotspots interception for the
 265 region. In this study, we select $PM_{2.5}$ as the fire emission tracer, as it is well known that $PM_{2.5}$ can
 266 be emitted by fires. CO can also serve as a tracer for fire influence for CO can be produced from
 267 incomplete combustion and has a long atmospheric lifetime. However, the range in CO is not as
 268 large as it is for $PM_{2.5}$. The variations of $PM_{2.5}$ during high influence fires can be over $100 \mu g/m^3$,
 269 which is more than double that of clean period, while CO varies much milder. Besides, the much
 270 more widespread $PM_{2.5}$ measurements compared to CO in Asia Pacific is another reason why
 271 $PM_{2.5}$ is chosen as the tracer for fire emissions. We then compared the number of interception fire
 272 hotspots with the measured $PM_{2.5}$ in Figure 5. In Figure 5a, correlation between the interception



number and $PM_{2.5}$ is not strong, indicating that identifying fire influence based on trajectory interception of a single fire hotspot is not effective. When we set the interception threshold to 50, the correlation significantly improves. This improvement may be due to larger and more fires generating more $PM_{2.5}$. Figure 5c illustrates how the correlations varies as the interception threshold changes. The correlation reaches it maximum at a threshold of 50. Therefore we set the interception threshold to be 50 in measuring the fire influence on $PM_{2.5}$ in Asia Pacific. Compared to the threshold of 20 in the North America proposed by Schneider et al. (2021), the interception threshold in Asia Pacific is higher, because the study area is much larger and the relative smaller scale of fires. This method eliminates fire hotspots that contribute minimally to $PM_{2.5}$ variations, while including as many measurements as possible.



283

Figure 5. (a) and (b) scatter distributions of $PM_{2.5}$ concentrations against the number of fire hotspots when interception threshold is set to be 1 and 50, respectively. (c) correlation coefficient between $PM_{2.5}$ and the number of fire hotspots as a function of the interception threshold.

Using the TFIM method, we isolate the station days influenced by fires. To estimating the fire-specific $PM_{2.5}$, we employed a random forest model for interpolation to estimate the



289 counterfactual $PM_{2.5}$ that is absence of fire influence, and then compare the $PM_{2.5}$ observation with
290 the counterfactual $PM_{2.5}$ to get the fire-specific $PM_{2.5}$.

291 With multi-source data of station days that are absence of fires, we generate the datasets for
292 machine learning model construction. There are totally 60 initial input variations, including 50
293 aerosol variables from MERRA2, MAIAC AOD, meteorological factors, land use, the NDVI and
294 the GDP data. We ranked the importance of these variables using random forest, with the most 15
295 influential variables in Figure 6a. The most influential variables for $PM_{2.5}$ that are absence of fire
296 is the surface black carbon mass (BCSMAS from MERRA2), followed by the surface mass
297 concentrations of various $PM_{2.5}$ components, like organic carbon and dust. Meteorological factors
298 contribute to explain variations in background $PM_{2.5}$. Temperature, pressure and humidity near
299 ground can affect the formation of particles by influencing on chemical actions between
300 precursors, while large-scale weather circulations also impact on pollutants transport and
301 accumulation through high level meteorological factors. In addition, other variations such as GDP
302 and NDVI also play a role in calculating background $PM_{2.5}$. GDP is expected to reflect the
303 economic conditions and background anthropogenic emissions among various regions, while
304 NDVI represents the vegetation cover status, which not only reflects the vegetation emissions but
305 also indicates the interception and deposition of $PM_{2.5}$ by vegetation. We then established an
306 estimation model using random forest with the 15 most influential input data to calculate the $PM_{2.5}$
307 that is absence of fire. The background $PM_{2.5}$ estimates derived from the model were compared
308 with observations, with an estimating R^2 of 0.8958 and RMSE of $0.3370 \mu\text{g}/\text{m}^3$ (Figure 6b). A
309 little under-estimation of the background $PM_{2.5}$ as it shows, the estimation has been highly
310 correlated with observations compared with the similar studies (Aguilera et al., 2021; 2023; Wei et
311 al., 2023).

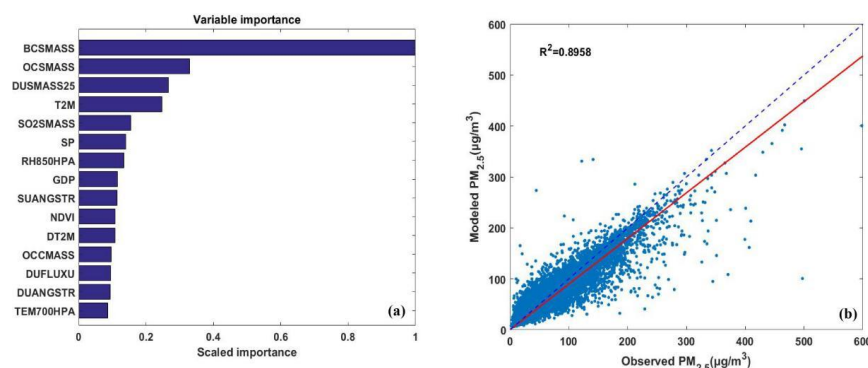


Figure 6. (a) Variation importance for the top 15 variables in estimating background PM_{2.5}; (b) Scatter distribution between modeled and observed PM_{2.5} that is absence of fire. Dashed blue lines represents the reference, and red line is the linear model fit.

The fire-specific PM_{2.5} was then estimated through subtracting the background PM_{2.5} that is absence of fire from the monitoring PM_{2.5}. Figure 7a and 7b show spatial distributions of the 8-year mean total PM_{2.5} and fire-specific PM_{2.5} in Asia Pacific, respectively. PM_{2.5} in Asia Pacific mostly has exceeded the health concentration standards for PM_{2.5} set by the WHO (annual average not exceeding 10 μg/m³). The highest mean concentrations for total PM_{2.5} are observed in northern India and Pakistan, followed by the Northeastern China, Indochina Peninsula, Mongolia and central India. To improve air quality, various measurements and particulate matter environmental standards have been implemented in countries of Asia Pacific, such as China's 'Air Pollution Prevention and Control Action Plan' since 2013, South Korea's enacting of the special act on the reduction and management of fine dust in 2018, India's launching of the National Clean Air Programme in 2019 and Thailand's amending the Enhancement and Conservation of National Environmental Quality Act in 2018, and so on. From 2014 to 2021, observed PM_{2.5} concentrations saw substantial decrease in various regions of Asia Pacific (Figure 9). The highest PM_{2.5} was monitored in EA during early period, but since 2018 PM_{2.5} in CA began to exceed that of EA. In contrast, NA and ESA have experienced lower annual average PM_{2.5} concentrations.

The spatial distribution of fire-specific PM_{2.5} is quite different with total PM_{2.5}, with highest concentrations appearing in Southeast Asia and Mongolia. As shown in Figure 4, fire hotspots number in SEA is more than twice as much as in other regions, which may partly explain the higher fire-specific PM_{2.5} in this region. Mongolia has a large area of semi-arid forests with grass understories. Forests those located in mid to high latitude areas and dominated by a few coniferous



tree species, are prone to a series of fire behaviors during droughts. Due to limited funding, firefighting efforts for forest fires in Mongolia are somewhat limited, leading to large-scale, long-duration forest and grassland fires during the dry season. Climate change, especially droughts, has intensified fire activities in Southern Siberia (including Mongolia), leading to a notable increase in fire numbers and shorter fire intervals (Hessl et al., 2016; Huang et al., 2024; Gui et al., 2024). As a result, higher fire-specific $PM_{2.5}$ can be found in the region of Asia Pacific. Besides, northern India is susceptible to fires before the monsoon and during the dry winter season, and northeastern and southwestern China are prone to forest fires in spring and autumn.

The annual average concentration of fire-specific $PM_{2.5}$ ranges from 2 to 8 $\mu g/m^3$, surging to between 2 and 15 $\mu g/m^3$ during the fire season. Areas where the concentration of fire-specific $PM_{2.5}$ surpasses 10 $\mu g/m^3$ encompass northern India, the northeastern and southwestern China, as well as several countries across SEA during fire seasons, as depicted in Figure 7 and 8. Contrary to the distribution of total $PM_{2.5}$, fire-specific $PM_{2.5}$ is notably higher in NA and ESA both in terms of annual average and during the fire season. In addition, fire-specific $PM_{2.5}$ saw an increase trend in NA since 2016, and in ESA since 2018, with this trend more pronounced during the fire season. In contrast, fire-specific $PM_{2.5}$ in EA and CA show slow decline. The total $PM_{2.5}$ has seen a significant decline thanks to efforts in controlling anthropogenic emissions from industry and transportation. However, fire-specific $PM_{2.5}$ decreases more slowly or even rebounds, leading to a gradual increase in the proportion of fire-specific $PM_{2.5}$ within total concentrations. In NA, the proportion during the fire season has grown from 0.2 to 0.3, while in ESA it has risen from 0.2 in 2018 to 0.4 in 2021. Proportions of fire-specific $PM_{2.5}$ in Malaysia, Cambodia and Brunei even exceeded 0.5 during the fire season. (Figure 8). The proportions in the EA and CA also display gradual upward trends.

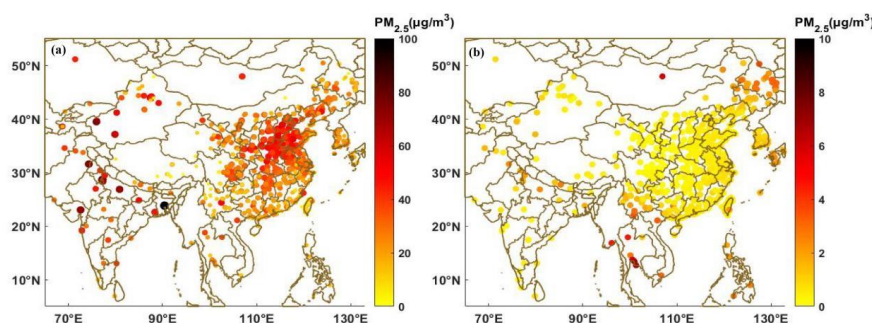
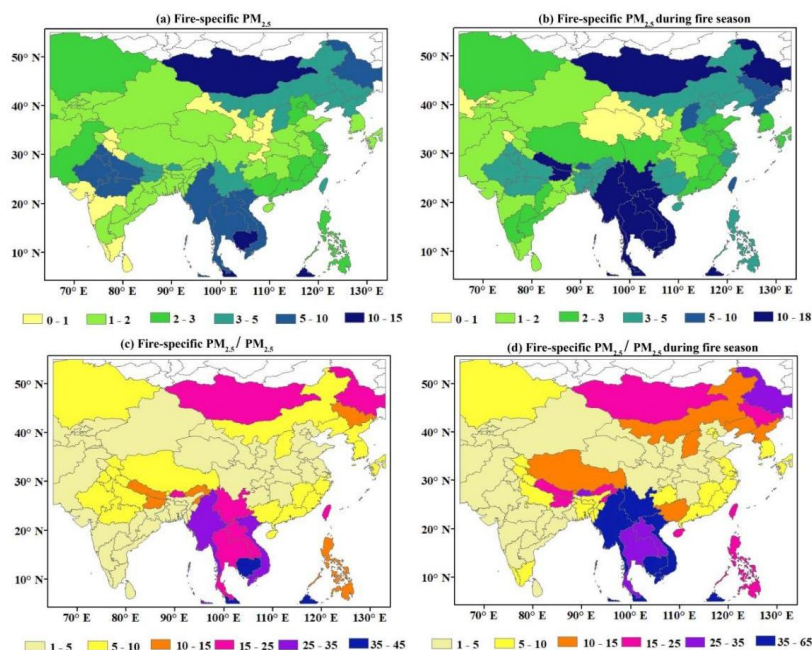


Figure 7. Distributions of (a) Mean $PM_{2.5}$ from all sources; (b) Mean fire-specific $PM_{2.5}$.



361

362 **Figure 8.** Regional averaged distributions of (a) annual mean and (b) fire season mean fire-specific
363 $PM_{2.5}$; Proportion of (c) annual mean and (d) fire season mean fire-specific $PM_{2.5}$ to total $PM_{2.5}$.

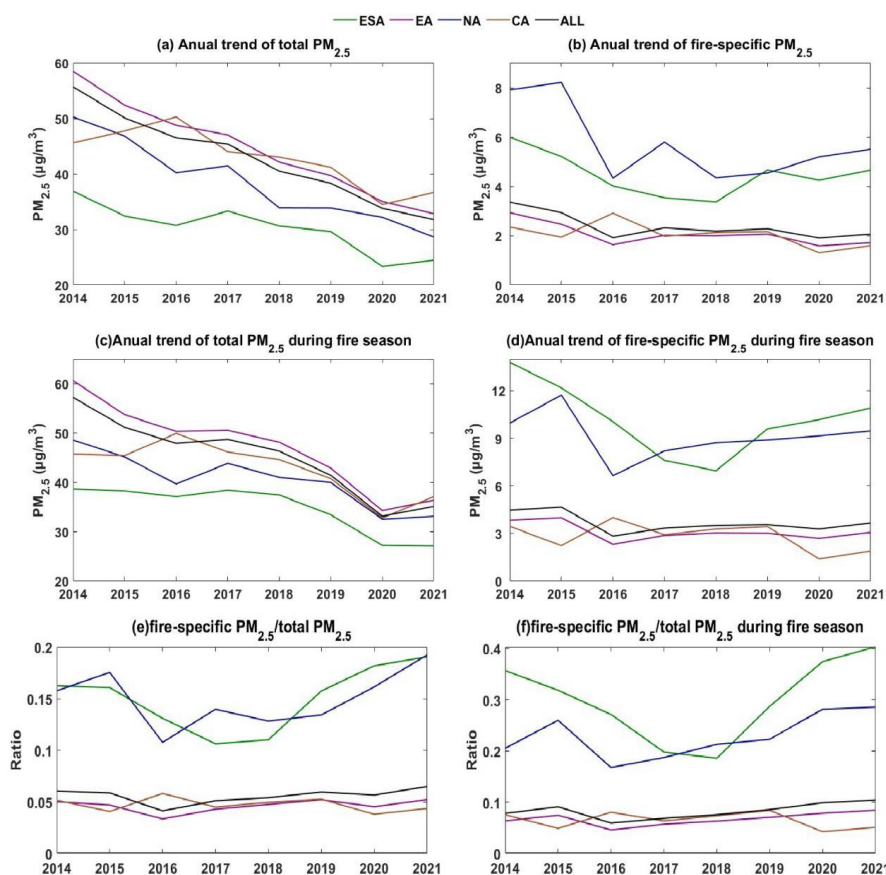


Figure 9. Temporal variations of (a) annual mean $PM_{2.5}$ and (b) fire season mean $PM_{2.5}$ in different regions; (c)(d) similar to (a)(b), but for fire-specific $PM_{2.5}$; (e)(f) similar to (a)(b), but for proportions of fire-specific $PM_{2.5}$ to total $PM_{2.5}$.

To illustrate the population exposure, we then calculated the population-weighted $PM_{2.5}$ and fire-specific $PM_{2.5}$ from 2014 to 2021 (Figure S1). Population-weighted $PM_{2.5}$ in different regions saw a significant decline during the 8 years, with reductions of 30.5% in ESA, 41.1% in EA, 31.4% in NA and 7.9% for CA, amounting to an overall decrease of 39.9% for the entire region. $PM_{2.5}$ concentrations are high in densely populated areas of CA, such as northern India, Bangladesh, and Pakistan (Figure S2), resulting in higher population-weighted $PM_{2.5}$. This indicates that population in CA is more likely to be exposed to $PM_{2.5}$. In EA, population-weighted $PM_{2.5}$ concentrations are higher in the east and lower in the west, which is consistent with the distribution of population density in the region. The distributions of population-weighted $PM_{2.5}$ in



377 ESA and NA are similar to their averaged $PM_{2.5}$. During fire seasons, distributions of population
378 exposure to $PM_{2.5}$ differ from those of total $PM_{2.5}$. Population-weighted fire-specific $PM_{2.5}$ in ESA
379 is higher than mean $PM_{2.5}$, indicating populations in ESA is more vulnerable to fire-specific $PM_{2.5}$
380 exposure. However, population-weighted $PM_{2.5}$ in CA is slightly lower than mean $PM_{2.5}$.

381 We then estimated the averted premature deaths due to changes in exposure to $PM_{2.5}$ from
382 eliminating fire emissions. Eliminating fire-specific $PM_{2.5}$ can avert approximately 58000
383 premature deaths annually in ESA, 90000 in EA, 157000 in CA and 29300 in NA. These account
384 for about 40.9%, 14.9%, 19.4%, and 24.1% of the total annual premature deaths attributed to
385 $PM_{2.5}$. During fire season, these proportions can rise to 57.7%, 19.5%, 21.6%, and 31.6%.
386 Distributions of premature deaths due to $PM_{2.5}$ in CA and NA (Figure 10) are closely aligned with
387 population distribution (Figure S2), because in these regions areas with higher population density
388 tend to expose in higher $PM_{2.5}$. The highest number of premature deaths attributed to fire-specific
389 $PM_{2.5}$ occur in Myanmar, Vietnam, northern India, and Pakistan, with notable increases during the
390 fire season in Thailand and southwestern China. Distributions of premature deaths attributed to
391 $PM_{2.5}$ relative to regional population proportions closely resembles the $PM_{2.5}$ distribution, with
392 areas exceeding 50 per 100000 mainly located in regions where annual mean $PM_{2.5}$ exceeds 40
393 $\mu g/m^3$. Similarly, the distribution of premature deaths caused by fire-specific $PM_{2.5}$ aligns closely
394 with $PM_{2.5}$ distribution (Figure 10d), with areas exceeding 20 per 100,000 predominantly found in
395 the fire-prone Southeast Asian Peninsula, Mongolia, and northeastern China. The number of
396 annual premature deaths due to $PM_{2.5}$ in the whole study region is around 1.7 million, accounting
397 for 47.2 per 100000 of the total population.

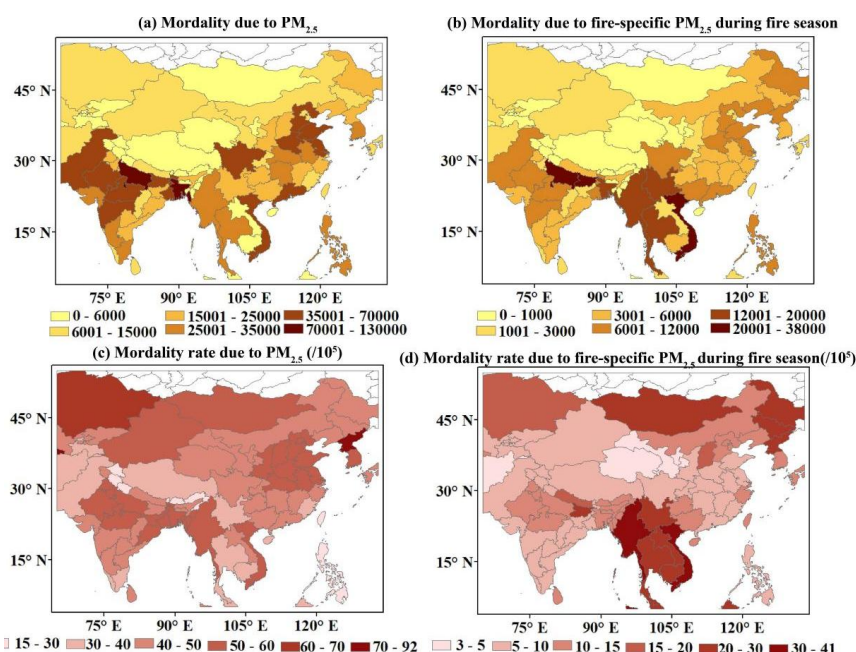


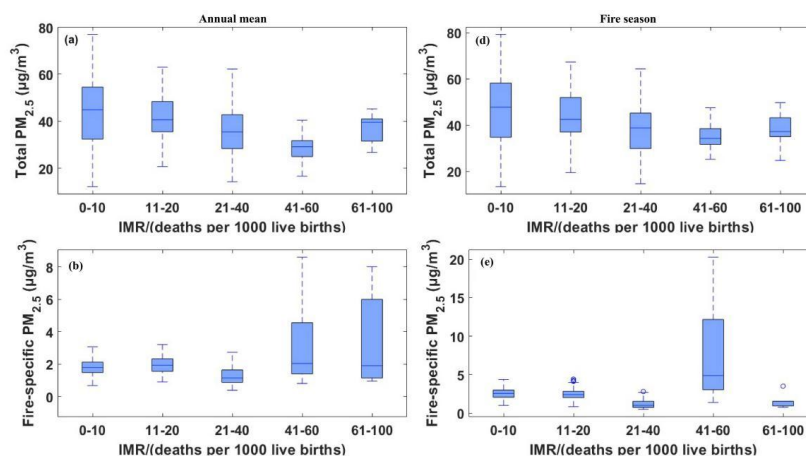
Figure 10. Distribution of premature deaths numbers due to (a) PM_{2.5} and (b) fire-specific PM_{2.5}, and the proportion of premature deaths relative to the local populations due to (c) PM_{2.5} and (d) fire-specific PM_{2.5}.

We further examined the poverty levels of Asia Pacific's population exposed to PM_{2.5}. Figure 11 illustrates total PM_{2.5} and fire-specific PM_{2.5} plotted against poverty proxy (IMR) data in Asia Pacific. For total PM_{2.5}, regions with IMR ≤ 60 show a gradual decrease in PM_{2.5} exposure levels as IMR values increase. In low IMR areas (IMR ≤ 10), the average PM_{2.5} (44.2 μg/m³) is significantly higher than that in regions with relatively higher IMR (41 ≤ IMR ≤ 60), where the PM_{2.5} averages at 28.3 μg/m³. In high IMR areas (IMR ≥ 61), the PM_{2.5} exposure level increases again to 37.0 μg/m³. While for fire-specific PM_{2.5} the trend is reversed, with higher IMR regions (IMR ≥ 40) are exposed to higher PM_{2.5}, while lower IMR regions (IMR < 40) experience relatively lower PM_{2.5}. During fire season, populations in regions with IMR ≥ 41 and ≤ 60 are exposed to the highest fire-specific PM_{2.5}.

It is found that populations in “not poor” areas (IMR < 40) are exposed to higher mean PM_{2.5} from all sources, but lower fire-specific PM_{2.5}. This indicates that PM_{2.5} pollution during the study period is primarily driven by economic and urban development. Conversely, “moderately poor” populations (41 ≤ IMR ≤ 60) experience lower total PM_{2.5} exposure, but higher fire-specific



416 $PM_{2.5}$ exposure. In “very poor” areas ($IMR \geq 61$), both total $PM_{2.5}$ and fire-specific $PM_{2.5}$ are
417 high, making populations in these areas more susceptible to health impact of $PM_{2.5}$.

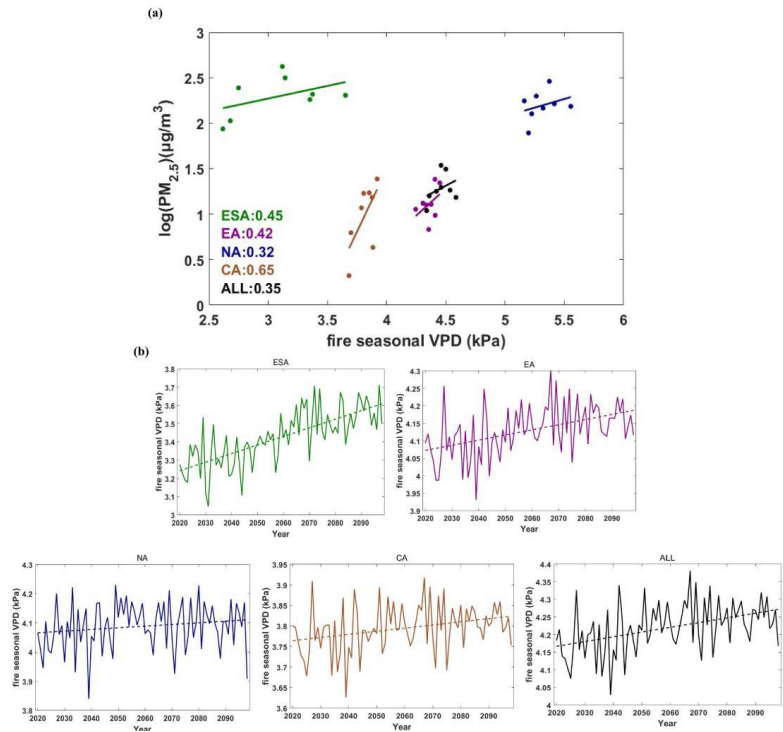


418
419 **Figure 11.** Annual mean (a) total $PM_{2.5}$ and (c) fire-specific $PM_{2.5}$ versus binned infant mortality
420 rate (IMR) values across the Asia Pacific. (b) (d) are similar to (a)(c), but for fire season mean.

421 Previous analysis indicates that fire-specific $PM_{2.5}$ in different regions have rebounded to
422 some extent, with more significant increase in ESA and NA. Whether this trend will continue or
423 be altered by occasional climate conditions is uncertain. Many studies have attempted to
424 understand the climate drivers of increased fire activities and how these factors may change in the
425 future (Abatzoglou and Williams, 2016; Xie et al., 2022; Barik et al., 2023; Burke et al., 2023; Gui
426 et al., 2024). These studies provide strong evidence that interannual variations in climate factors
427 are drivers of fire activities and changes in fire-specific $PM_{2.5}$. Based on future change of these
428 climate drivers predicted by GCMs, assuming no intervention, fire activities may increase with
429 global warming. With numerical model simulation, researches reveal that fire-specific $PM_{2.5}$ will
430 see rise in the future. To corroborate the future changes in fire-specific $PM_{2.5}$ of Asia Pacific, we
431 calculated mean VPD during fire season for different regions, and relate these values to
432 fire-specific $PM_{2.5}$. It is obvious that VPD is positively related to log of fire-specific $PM_{2.5}$ (Figure
433 13a). Climate drivers can explain 35% of fire-specific $PM_{2.5}$ variations in Asia Pacific, with
434 variation in CA most sensitive to VPD (65%). The multi-model ensemble mean of 34 GCM
435 projections indicates a future increasing trend in VPD, with a pronounced rise in ESA, followed
436 by EA and CA, while the increase is weaker in NA. These results suggest that the emerging
437 growth trend of fire-specific $PM_{2.5}$ in Asia Pacific is likely to continue under the influence of



438 future climate change. For more dynamic and spatially detailed characteristics, more data will
439 have to be integrated into modelling calculations to better understand the evolution of fire
440 occurrences and pollutants release under future climate impacts.



441
442 **Figure 12.** (a) Interannual variations of vapor pressure deficit (VPD) versus the log of averaged
443 fire-specific PM_{2.5} during fire season; (b) future VPD derived from multi-model ensemble mean of
444 34 GCM projections

445 4 Conclusion and discussion

446 In this study, we explored the contribution of forest and vegetation fires to air quality and
447 public health across the Asia Pacific. We isolate fire-specific PM_{2.5} from the monitoring data for
448 Asia Pacific using TFIM and spatiotemporal interpolation in this study. One advantage of this
449 dataset is that it is driven by monitoring concentrations rather than relying on emission databases,
450 which may probably ignore contributions of pollutants from smaller-scale fire emissions, and
451 carry considerable uncertainty, especially with the evident underestimation of agricultural fire
452 emissions. Moreover, this method offers reliability and timeliness, effectively saving
453 computational resources and storage space for isolating fire-related air pollution.



454 Our analysis reveals geographical disparities in population exposure to $PM_{2.5}$ and fire-related
455 air pollution in Asia Pacific. Thanks to the the establishment of $PM_{2.5}$ air quality standards and
456 pollution control measurement by countries, $PM_{2.5}$ population exposure saw an obvious declining
457 trend from 2014 to 2021 in Asia Pacific, with population-weighted $PM_{2.5}$ in 2021 reduced by
458 39.9% compared to 2014. High $PM_{2.5}$ concentrations are observed in EA and CA, concentrated in
459 densely populated areas, leading to substantially higher population-weighted concentrations than
460 mean $PM_{2.5}$. In contrast, fire-specific $PM_{2.5}$ decreased in the early years but began to reverse
461 recently in Asia Pacific. ESA and NA experienced the most obvious increase in fire-specific $PM_{2.5}$
462 in recent years, while EA and CA saw a slight increase. As a result, a gradual increase in the
463 proportion of fire-specific $PM_{2.5}$ within total concentrations can be observed.

464 We found that fire-related $PM_{2.5}$ could pose a significant public health threat in Asia Pacific,
465 contributing to approximately 334,300 premature deaths each year. The annual disease burden due
466 to $PM_{2.5}$ exposure can be reduced by 40.9%, 14.9%, 19.4%, and 24.1% in ESA, EA, CA, and NA,
467 respectively, averting 58,000, 90,000, 157,000, and 29,300 premature deaths. It is important to
468 note that our calculations do not account for the potentially higher toxicity of fire-specific $PM_{2.5}$
469 compared to other sources, which could lead to an even greater number of premature deaths and
470 related illnesses. Using infant mortality rates as a poverty proxy, we found that populations in
471 Asia Pacific are disproportionately exposed to $PM_{2.5}$. Populations in “not poor” areas ($IMR \leq 40$)
472 are exposed to higher total $PM_{2.5}$, while poor populations are more vulnerable to health impacts of
473 fire-specific $PM_{2.5}$. Our study indicates that the fire-related air pollution is also a serious issue in
474 many poverty areas, yet it receives less attention. This situation warrants further investigation to
475 explore the underlying causes and characteristics, ultimately providing more scientific evidence
476 for effective management strategies. Based on the positive correlation between VPD and
477 fire-specific $PM_{2.5}$, the study suggests that without further regulatory and policy intervention, the
478 emerging growth trend in fire-specific $PM_{2.5}$ in Asia Pacific is likely to continue under the
479 influence of future climate change.

480 Interestingly, the increasing trend in fire-specific $PM_{2.5}$ appears inconsistent with the
481 declining trend in the number of fire points in Asia Pacific. In earlier years, vegetation fires in the
482 region were dominated by agricultural fires, characterized with smaller-scale burning areas but



more fire point numbers. Countries have implemented various policies to reduce agricultural fires, such as China's measures to minimize straw burning and Thailand's alternative energy development plans, like zero-burning policy. The enforcement of these policies has, to some extent, reduced fire point numbers and emissions from agricultural fires in Asia Pacific. However, fire emissions in the region are also influenced by wildfire emissions related to climate change. Wildfires usually occur in natural vegetation and are characterized by larger-scale burning areas that are more challenging to extinguish. As a result, the emissions per unit of biomass burned in wildfires far exceed those from agricultural fires. To explain the inconsistent of changes in fire point numbers and emissions, it is proposed that while emissions from agriculture fires are decreasing, the increasing emissions from natural wildfires driven by climate change are gradually becoming dominant source of fire-specific $PM_{2.5}$ in Asia Pacific. This hypothesis may be further verified in the future studies.

This study indicate that the contributions of fire-specific $PM_{2.5}$ to air quality and health impact are becoming increasingly significant and deserve more attention when developing air pollution standards and control measurements in Asia Pacific. These variations suggest that the decreases in pollutant concentrations from traffic and industrial sources and the associated health benefits may be offset by increases in pollutant concentrations from fires. Measures to reduce fires may be a significant yet under-recognized option for effeciently improving air quality and averting the related premature deaths.

Data Available Statement

Air quality observation data can be acquired from <http://openaq.org/> and <http://www.cnemc.cn/en/>. The ERA5 data can be respectively downloaded from <https://cds.climate.copernicus.eu/cdsapp#!/dataset/reanalysis-era5-pressure-levels>. The fire point data are available at <https://earthdata.nasa.gov/firms>. The health data can be accessed in <http://ghdx.healthdata.org/gbd-results-tool>. The infant mortality rates data can be found at <https://www.earthdata.nasa.gov/data/catalog/sedac-ciesin-sedac-pmp-imr-v2.01-2.01>. The Coupled Model Intercomparison Project Phase 6 data can be get from <https://aims2.llnl.gov/search/cmip6/>. The aerosol optical depth data are available at <https://www.earthdata.nasa.gov/data/catalog/lancemodis-mcd19a2n-6.1nrt> and



512 <https://disc.gsfc.nasa.gov/datasets?project=MERRA-2>. The landuse data can be accessed in
513 <https://lpdaac.usgs.gov/products/mcd12q1v006/>. And the population data can be found at
514 <https://landscan.ornl.gov/>.

515 **Author contributions.** HL, MX and NW conceived the study, designed the experiments, conducted
516 the data isolation and prepared the initial draft manuscript. JJ, JY and KL collected the data and
517 assessed the health impacts of air pollution. HL, BL and BZ perform the analysis, engaged in
518 constructive discussions, reviewed and edited the manuscript. HL, MX and BL secured financial
519 support for the project leading to this publication. DM and MX provided additional manuscript reviews.

520 **Competing Interest:** The authors declare no conflict of interest.

521 **Financial support:** This work was supported by the National Natural Science Foundation of China
522 (42205186, 42275102), the Chongqing Natural Science Foundation (cstc2021jcyj-msxmX1007,
523 2024NSCQ-KJFZMSX0258), Special Science and Technology Innovation Program for Carbon Peak
524 and Carbon Neutralization of Jiangsu Province (BE2022612), the key technology research and
525 development of Chongqing Meteorological Bureau (YWJSGG-202215; YWJSGG-202303) and the
526 research start-up fund for the talented person recruitment of Nanjing Normal University
527 (184080H201B57).

528 Reference

- 529 Abatzoglou, J. T.; Williams, A. P., (2016). Impact of anthropogenic climate change on wildfire across western US
530 forests. *Proceedings of the National Academy of Sciences*, 113, (42), 11770-11775.
- 531 Aguilera, R., Corringham, T., Gershunov, A., Benmarhnia, T., (2021). Wildfire smoke impacts respiratory health
532 more than fine particles from other sources: observational evidence from Southern California. *Nat.*
533 *Commun.* 12 (1), 1–8.
- 534 Aguilera R, Luo N, Basu R, Wu J, Clemesha R, Gershunov A, Benmarhnia T., (2022). A novel ensemble-based
535 statistical approach to estimate daily wildfire-specific PM_{2.5} in California (2006-2020). *Environ Int.* 2023
536 Jan;171:107719. doi: 10.1016/j.envint.2022.107719. Epub Dec 24. PMID: 36592523; PMCID:
537 PMC10191217.
- 538 Barbier, E. B.; Hochard, J. P., (2019). Poverty-Environment Traps. *Environmental and Resource Economics*, 74,
539 (3), 1239-1271.
- 540 Barik, A.; Baidya Roy, S., (2023). Climate change strongly affects future fire weather danger in Indian forests.
541 *Communications Earth & Environment*, 4, (1), 452.
- 542 Barlow, M.; Zaitchik, B.; Paz, S.; Black, E.; Evans, J.; Hoell, A., (2016). A Review of Drought in the Middle East
543 and Southwest Asia. *Journal of Climate*, 29, (23), 8547-8574.



- 544 Biswas, S.; Vadrevu, K. P.; Lwin, Z. M.; Lasko, K., & Justice, C. O. (2015). Factors controlling vegetation fires in
545 protected and non-protected areas of Myanmar. *PLoS One*, 10, e0124346.
546 <https://doi.org/10.1371/journal.pone.0124346>.
- 547 Burke, M.; Childs, M. L.; de la Cuesta, B.; Qiu, M.; Li, J.; Gould, C. F.; Heft-Neal, S.; Wara, M., (2023). The
548 contribution of wildfire to PM_{2.5} trends in the USA. *Nature*, 622, (7984), 761-766.
- 549 Burnett, R.; Chen, H.; Szyszkowicz, M.; Fann, N.; Hubbell, B.; Pope, C. A.; Apte, J. S.; Brauer, M.; Cohen, A.;
550 Weichenthal, S.; Coggins, J.; Di, Q.; Brunekreef, B.; Frostad, J.; Lim, S. S.; Kan, H.; Walker, K. D.;
551 Thurston, G. D.; Hayes, R. B.; Lim, C. C.; Turner, M. C.; Jerrett, M.; Krewski, D.; Gapstur, S. M.; Diver,
552 W. R.; Ostro, B.; Goldberg, D.; Crouse, D. L.; Martin, R. V.; Peters, P.; Pinault, L.; Tjepkema, M.; van
553 Donkelaar, A.; Villeneuve, P. J.; Miller, A. B.; Yin, P.; Zhou, M.; Wang, L.; Janssen, N. A. H.; Marra,
554 M.; Atkinson, R. W.; Tsang, H.; Quoc Thach, T.; Cannon, J. B.; Allen, R. T.; Hart, J. E.; Laden, F.;
555 Cesaroni, G.; Forastiere, F.; Weinmayr, G.; Jaensch, A.; Nagel, G.; Concin, H.; Spadaro, J. V., (2018).
556 Global estimates of mortality associated with long-term exposure to outdoor fine particulate matter.
557 *Proceedings of the National Academy of Sciences*, 115, (38), 9592-9597.
- 558 Bytnerowicz, A.; Hsu, Y.-M.; Percy, K.; Legge, A.; Fenn, M. E.; Schilling, S.; Frączek, W.; Alexander, D. (2016).
559 Ground-Level Air Pollution Changes during a Boreal Wildland Mega-Fire. *Sci. Total Environ.* 572,
560 755–769.
- 561 Campbell-Lendrum, D.; Prüss-Ustün, A., (2019). Climate change, air pollution and noncommunicable diseases.
562 *Bulletin of the World Health Organization*, 97, (2), 160-161.
- 563 Chen, G., Guo, Y., Yue, X., Tong, S., Gasparrini, A., Bell, M.L., Armstrong, B., Schwartz, J., Jaakkola, J.J.K.,
564 Zanobetti, A., Lavigne, E., Nascimento Saldiva, P.H., Kan, H., Royé, D., Milojevic, A., Overcenco, A.,
565 Urban, A., Schneider, A., Entezari, A., Vicedo-Cabrera, A.M., Zeka, A., Tobias, A., Nunes, B., Alahmad,
566 B., Forsberg, B., Pan, S.-C., Iñiguez, C., Ameling, C., De la Cruz Valencia, C., Åström, C., Houthuijs,
567 D., Van Dung, D., Samoli, E., Mayvaneh, F., Sera, F., Carrasco-Escobar, G., Lei, Y., Orru, H., Kim, H.,
568 Holobaca, I.-H., Kysely, J., Teixeira, J.P., Madureira, J., Katsouyanni, K., Hurtado-Díaz, M.,
569 Maasikmets, M., Ragettli, M.S., Hashizume, M., Stafoggia, M., Pascal, M., Scortichini, M., de Sousa
570 Zanotti Stagliorio Coelho, M., Valdés Ortega, N., Rytí, N.R.I., Scovronick, N., Matus, P., Goodman, P.,
571 Garland, R.M., Abrutzky, R., Garcia, S.O., Rao, S., Fratianni, S., Dang, T.N., Colistro, V., Huber, V.,
572 Lee, W., Seposo, X., Honda, Y., Guo, Y.L., Ye, T., Yu, W., Abramson, M.J., Samet, J.M., & Li, S.
573 (2021). Mortality risk attributable to wildfire-related PM_{2.5} pollution: a global time series study in 749
574 locations. *The Lancet Planetary Health*, 5, e579-e587
- 575 Climate & Clean Air Coalition. (n.d.). Air pollution measures for Asia and the Pacific. Retrieved November 25,
576 2024, from <https://www.ccacoalition.org/content/air-pollution-measures-asia-and-pacific>.
- 577 Dreessen, J.; Sullivan, J.; Delgado, R. (2015). Observations and Impacts of Transported Canadian Wildfire Smoke
578 on Ozone and Aerosol Air Quality in the Maryland Region on June 9-12, *J. Air Waste Manag. Assoc.*
- 579 Du X, Chen R, Kan H. (2024). Challenges of Air Pollution and Health in East Asia. *Curr Environ Health Rep.*
580 Jun;11(2):89-101. doi: 10.1007/s40572-024-00433-y. Epub 2024 Feb 7. PMID: 38321318.
- 581 Fairburn, J.; Schüle, S. A.; Dreger, S.; Karla Hilz, L.; Bolte, G., (2019). Social Inequalities in Exposure to Ambient
582 Air Pollution: A Systematic Review in the WHO European Region. In *International Journal of*
583 *Environmental Research and Public Health*. Vol. 16.



- 584 Feng, X., Mao, R., Gong, D., Zhao, C., Wu, C., Zhao, C., Wu, G., Lin, Z., Liu, X., Wang, K., and Sun, Y. (2020).
585 Increased Dust Aerosols in the High Troposphere Over the Tibetan Plateau From 1990s to 2000s ,
586 Journal of Geophysical Research: Atmospheres, 125(13): 1-11.
- 587 Gelaro, R., and Coauthors. (2017). The Modern-Era Retrospective Analysis for Research and Applications,
588 Version 2 (MERRA-2). J. Climate, 30, 5419–5454, <https://doi.org/10.1175/JCLI-D-16-0758.1>.
- 589 Giannadaki D, Giannakis E, Pozzer A, Lelieveld J. (2018). Estimating health and economic benefits of reductions
590 in air pollution from agriculture. Sci Total Environ. May 1;622-623:1304-1316. doi:
591 10.1016/j.scitotenv.2017.12.064. Epub 2017 Dec 13. PMID: 29890597.
- 592 Giglio, L.; Descloitres, J.; Justice, C. O.; Kaufman, Y. J. (2003). An Enhanced Contextual Fire Detection
593 Algorithm for MODIS. Remote Sens. Environ. 87, 273–282.
- 594 Gui, K.; Zhang, X.; Che, H.; Li, L.; Zheng, Y.; Zhao, H.; Zeng, Z.; Miao, Y.; Wang, H.; Wang, Z.; Wang, Y.; Ren,
595 H.-L.; Li, J.; Zhang, X., (2024). Future climate-driven escalation of Southeastern Siberia wildfires
596 revealed by deep learning. npj Climate and Atmospheric Science, 7, (1), 263.
- 597 He, Q., Gu, Y., and Zhang, M. (2020). Spatiotemporal trends of PM_{2.5} concentrations in central China from 2003
598 to 2018 based on MAIAC-derived high-resolution data [J], Environment International, 137: 105536.
- 599 Hessel, A. E.; Brown, P.; Byambasuren, O.; Cockrell, S.; Leland, C.; Cook, E.; Nachin, B.; Pederson, N.; Saladyga,
600 T.; Suran, B., (2016) Fire and climate in Mongolia (1532–2010 Common Era). Geophysical Research
601 Letters, 43, (12), 6519-6527.
- 602 Huang, R.; Liu, Y.; Du, Z.; Chen, J.; Huangfu, J., (2017). Differences and links between the East Asian and South
603 Asian summer monsoon systems: Characteristics and Variability. Advances in Atmospheric Sciences ,
604 34, (10), 1204-1218.
- 605 Huang, X.; Xue, L.; Wang, Z.; Liu, Y.; Ding, K.; Ding, A., (2024) Escalating Wildfires in Siberia Driven by
606 Climate Feedbacks Under a Warming Arctic in the 21st Century. AGU Advances, 5, (4),
607 e2023AV001151.
- 608 Jia, R., Min, L., Liu, Y., Qingzhe, Z., Hua, S., Wu, C., and Shao, T. (2019). Anthropogenic Aerosol Pollution over
609 the Eastern Slope of the Tibetan Plateau [J], Advances in Atmospheric Sciences, 36(9): 847-862.
- 610 Justice, C. O.; Giglio, L.; Roy, D.; Boschetti, L.; Csiszar, I.; Davies, D.; Korontzi, S.; Schroeder, W.; O’Neal, K.;
611 Morissette, J. (2011). MODIS-Derived Global Fire Products. In Land Remote Sensing and Global
612 Environmental Change: NASA’s Earth Observing System and the Science of ASTER and MODIS,
613 Ramachandran, B.; Justice, C. O.; Abrams, M. J., Eds.; Springer New York: New York, NY,
614 pp661–679.
- 615 Korsiak, Jill & Pinault, Lauren & Christidis, Tanya & Burnett, Richard & Abrahamowicz, Michal & Weichenthal,
616 Scott. (2022). Long-term exposure to wildfires and cancer incidence in Canada: a population-based
617 observational cohort study. The Lancet Planetary Health. 6. e400-e409.
618 10.1016/S2542-5196(22)00067-5.
- 619 Landis, M. S.; Edgerton, E. S.; White, E. M.; Wentworth, G. R.; Sullivan, A. P.; Dillner, A. M. (2018). The Impact
620 of the 2016 Fort McMurray Horse River Wildfire on Ambient Air Pollution Levels in the Athabasca Oil
621 Sands Region, Alberta, Canada. Sci. Total Environ. 618, 1665–1676.



- 622 Lelieveld, J., Evans, J., Fnais, M. et al. (2015). The contribution of outdoor air pollution sources to premature
623 mortality on a global scale. *Nature* 525, 367–371 <https://doi.org/10.1038/nature15371>.
- 624 Lelieveld, J.; Pozzer, A.; Pöschl, U.; Fnais, M.; Haines, A.; Münzel, T., (2020). Loss of life expectancy from air
625 pollution compared to other risk factors: a worldwide perspective. *Cardiovascular Research*, 116, (11),
626 1910-1917.
- 627 Li, L., Franklin, M., Girguis, M., Lurmann, F., Wu, J., Pavlovic, N., Breton, C., Gilliland, F., and Habre, R. (2020).
628 Spatiotemporal imputation of MAIAC AOD using deep learning with downscaling [J], *Remote Sensing*
629 *of Environment*, 237: 111584.
- 630 Lyapustin, A., Wang, Y., Korkin, S., and Huang, D. (2018). MODIS Collection 6 MAIAC algorithm, *Atmos.*
631 *Meas. Tech.*, 11, 5741–5765, <https://doi.org/10.5194/amt-11-5741-2018>.
- 632 McDuffie, E. E.; Martin, R. V.; Spadaro, J. V.; Burnett, R.; Smith, S. J.; O'Rourke, P.; Hammer, M. S.; van
633 Donkelaar, A.; Bindle, L.; Shah, V.; Jaeglé, L.; Luo, G.; Yu, F.; Adeniran, J. A.; Lin, J.; Brauer, M.,
634 (2021). Source sector and fuel contributions to ambient PM_{2.5} and attributable mortality across multiple
635 spatial scales. *Nature Communications*, 12, (1), 3594.
- 636 Phairuang, W., Hata, M., & Furuuchi, M. (2017). Influence of agricultural activities, forest fires and
637 agro-industries on air quality in Thailand. *Journal of Environmental Sciences*, 52, 85–97.
638 <https://doi.org/10.1016/j.jes.2016.02.007>.
- 639 Qin, Y.; Wang, H.; Wang, Y.; Lu, X.; Tang, H.; Zhang, J.; Li, L.; Fan, S., (2024). Wildfires in Southeast Asia
640 pollute the atmosphere in the northern South China Sea. *Science bulletin*, 69, (8), 1011-1015.
- 641 Reddington, C. L., Conibear, L., Robinson, S., Knote, C., Arnold, S. R., & Spracklen, D. V. (2021). Air pollution
642 from forest and vegetation fires in Southeast Asia disproportionately impacts the poor. *GeoHealth*, 5,
643 e2021GH000418. <https://doi.org/10.1029/2021GH000418>.
- 644 Romanov, A. A.; Tamarovskaya, A. N.; Gusev, B. A.; Leonenko, E. V.; Vasiliev, A. S.; Krikunov, E. E., (2022)
645 Catastrophic PM_{2.5} emissions from Siberian forest fires: Impacting factors analysis. *Environmental*
646 *Pollution*, 306, 119324.
- 647 Schneider, S. R., Lee, K., Santos, G., & Abbatt, J. P. D. (2021). Air quality data approach for defining wildfire
648 influence: Impacts on PM_{2.5}, NO₂, CO, and O₃ in western Canadian cities. *Environmental Science &*
649 *Technology*, 55(20), 13709–13717. <https://doi.org/10.1021/acs.est.1c04042>.
- 650 Schneider, S. R., Shi, B., & Abbatt, J. P. D. (2024). The measured impact of wildfires on ozone in Western Canada
651 from 2001 to 2019. *Journal of Geophysical Research: Atmospheres*, 129, e2023JD038866.
652 <https://doi.org/10.1029/2023JD038866>.
- 653 Tornevi A, Andersson C, Carvalho AC, Langner J, Stenfors N, Forsberg B. (2021). Respiratory Health Effects of
654 Wildfire Smoke during Summer of 2018 in the Jämtland Härjedalen Region, Sweden. *Int J Environ Res*
655 *Public Health*. Jun 29;18(13):6987. doi: 10.3390/ijerph18136987. PMID: 34210080; PMCID:
656 PMC8297091.
- 657 Wei, J.; Wang, J.; Li, Z.; Kondragunta, S.; Anenberg, S.; Wang, Y.; Zhang, H.; Diner, D.; Hand, J.; Lyapustin, A.;
658 Kahn, R.; Colarco, P.; da Silva, A.; Ichoku, C., (2023). Long-term mortality burden trends attributed to



- 659 black carbon and PM_{2.5} from wildfire emissions across the continental USA from 2000 to 2020: a deep
660 learning modelling study. *The Lancet Planetary Health*, 7, (12), e963-e975.
- 661 Wiedinmyer, Christine, Brad Quayle, Chris Geron, Angle Belote, Don McKenzie, Xiaoyang Zhang, Susan O'Neill,
662 and Kristina Klos Wynne. (2006). Estimating Emissions from Fires in North America for Air Quality
663 Modeling, *Atmospheric Environment*, 40, 3419-32.
- 664 Wiedinmyer, C., S. K. Akagi, R. J. Yokelson, L. K. Emmons, J. A. Al-Saadi, J. J. Orlando, and A. J. Soja. (2011).
665 The Fire Inventory from NCAR (FINN): A High Resolution Global Model to Estimate the Emissions
666 from Open Burning, *Geoscientific Model Development*, 4, doi:10.5194/gmd-4-625-2011.
- 667 Wiedinmyer, C., Kimura, Y., McDonald-Buller, E. C., Emmons, L. K., Buchholz, R. R., Tang, W., Seto, K.,
668 Joseph, M. B., Barsanti, K. C., Carlton, A. G., and Yokelson, R. (2023). The Fire Inventory from NCAR
669 version 2.5: an updated global fire emissions model for climate and chemistry applications, *Geosci.*
670 *Model Dev.*, 16, 3873–3891, <https://doi.org/10.5194/gmd-16-3873-2023>.
- 671 World Bank. (2016). East Asia and Pacific cities: Expanding opportunities for the urban poor.
672 <https://openknowledge.worldbank.org/handle/10986/25074>.
- 673 World Health Organization. "Ambient (Outdoor) Air Quality and Health." World Health Organization, 24 Oct.
674 2024, [https://www.who.int/news-room/fact-sheets/detail/ambient-\(outdoor\)-air-quality-and-health](https://www.who.int/news-room/fact-sheets/detail/ambient-(outdoor)-air-quality-and-health).
- 675 World Health Organization. (2022). World Health Statistics 2022.
676 <https://www.who.int/data/gho/publications/world-health-statistics>.
- 677 Xie, Y.; Lin, M.; Decharme, B.; Delire, C.; Horowitz, L. W.; Lawrence, D. M.; Li, F.; Séférian, R., (2022).
678 Tripling of western US particulate pollution from wildfires in a warming climate. *Proceedings of the*
679 *National Academy of Sciences*, 119, (14), e2111372119.
- 680 Xie, Y.; Zhou, M.; Hunt, K. M. R.; Mauzerall, D. L., (2024). Recent PM_{2.5} air quality improvements in India
681 benefited from meteorological variation. *Nature Sustainability*, 7, (8), 983-993.
- 682 Xu, F.; Huang, Q.; Yue, H.; Feng, X.; Xu, H.; He, C.; Yin, P.; Bryan, B. A., (2023b). The challenge of population
683 aging for mitigating deaths from PM_{2.5} air pollution in China. *Nature Communications*, 14, (1), 5222.
- 684 Xu, R., Ye, T., Yue, X. et al. (2023a). Global population exposure to landscape fire air pollution from 2000 to
685 2019. *Nature* 621, 521–529. <https://doi.org/10.1038/s41586-023-06398-6>.
- 686 Xue, T., Geng, G., Li, J., Han, Y., Guo, Q., Kelly, F. J., Wooster, M. J., Wang, H., Jiangtulu, B., Duan, X., Wang,
687 B., and Zhu, T. (2021). Associations between exposure to landscape fire smoke and child mortality in
688 low-income and middle-income countries: a matched case-control study, *The Lancet Planetary Health*, 5,
689 e588-e598, 10.1016/S2542-5196(21)00153-4,.
- 690 Yin, S., (2020). Biomass burning spatiotemporal variations over South and Southeast Asia. *Environment*
691 *International*, 145, 106153.
- 692 Yue, H.; He, C.; Huang, Q.; Yin, D.; Bryan, B. A., (2020). Stronger policy required to substantially reduce deaths
693 from PM_{2.5} pollution in China. *Nature Communications*, 11, (1), 1462
- 694 Zhang, Q.; Zheng, Y.; Tong, D.; Shao, M.; Wang, S.; Zhang, Y.; Xu, X.; Wang, J.; He, H.; Liu, W.; Ding, Y.; Lei,
695 Y.; Li, J.; Wang, Z.; Zhang, X.; Wang, Y.; Cheng, J.; Liu, Y.; Shi, Q.; Yan, L.; Geng, G.; Hong, C.; Li,



- 696 M.; Liu, F.; Zheng, B.; Cao, J.; Ding, A.; Gao, J.; Fu, Q.; Huo, J.; Liu, B.; Liu, Z.; Yang, F.; He, K.; Hao,
697 J., D. (2019). rivers of improved PM_{2.5} air quality in China from 2013 to 2017. Proceedings of the
698 National Academy of Sciences, 116, (49), 24463-24469.
- 699 Zheng, H.; Xue, L.; Ding, K.; Lou, S.; Wang, Z.; Ding, A.; Huang, X., (2023). ENSO-Related Fire Weather
700 Changes in Southeast and Equatorial Asia: A Quantitative Evaluation Using Fire Weather Index. Journal
701 of Geophysical Research: Atmospheres, 128, (21), e2023JD039688.
- 702 Zhu, J., Xia, X., Che, H., Wang, J., Zhang, J., & Duan, Y. (2016). Study of aerosol optical properties at Kunming
703 in southwest China and long-range transport of biomass burning aerosols from North Burma.
704 Atmospheric Research, 169, 237–247. <https://doi.org/10.1016/j.atmosres.2015.10.012>.